2020 IEEE/RSJ International Conference on Intelligent Robots and Systems (IROS)
October 25-29, 2020, Las Vegas, NV, USA (Virtual)

Design of a new electroactive polymer based continuum actuator for endoscopic surgical robots

Q.JACQUEMIN[1], Q.SUN[1,2], D.THUAU[2], E.MONTEIRO[1], S.TENCE-GIRAULT[1,3] and N.MECHBAL[1‡]

Abstract

This paper presents a smart continuum actuator based on a promising class of materials: ElectroActive polymer (EAP). Indeed these polymers undergo dimensional change in response to an applied electrical field and could be integrated directly in an endoscopic robot structure. We focuses on one of such materials, an electrostrictive polymer, for its valuable strain performances. An analytical model leading to the development of an experimental analysis of such a material in an attempts to overcome the technical gap of their integration into a multilayer composite sheet to perform robotic actuation is the subject of this article.

1. INTRODUCTION

This paper describes a novel continuum actuator for endoscopic robots applications in surgery. It is part of a larger project led by Tenon hospital urology service in Paris towards the realization of a cystoscopic robot. To improve the automation level of the medical field made possible by the development of miniaturized components, we have to upgrade traditional tools. Indeed, actual endoscopic devices are made up of wire-actuated mechanical actuators and a distal tip camera as a unique embedded sensor with the surgeon's wrist achieving the roll motion to reach the surface of the entire targeted organ. Instead, partial or full automation of these tools would free surgeons from time-consuming tasks and help them achieve complicated gestures via remote control and augmented reality. From embedded micro-motor actuated joints to autonomous drug capsules [1],[2], over the past few years, scientists have been studying several new models of endoscopic actuators. The applicability of each of these models depends on the kind of surgery. Due to the micro-scale environment, we must choose miniaturized actuators for the endoscopic robots used in urology or ENT (Ears Nose Throat) related surgery. Consequently, research on continuum actuators using smart materials has emerged as these can be directly integrated on the robot shape. Contrary to the traditional joint and link rigid structures, continuum soft actuators can reach infinite degrees of freedom. For instance, shape memory alloys and Electro Active Polymers (EAP) are two emerging families of promising materials for surgical automated actuators where biocompatibility, high strains and micro-scaled dimension are desired features [3], [4] and [5]. EAPs can be classified into two categories: ionic EAPs and electronic EAPs. The electrical bending activation of ionic EAPs is due to the migration of ions or electrically charged molecules (figure 1 a) whereas electronic EAPs are activated by applied electric fields and various polarization effects (Coulombs forces, ferroelectricity or relaxor-ferroelectricity) (figure 1 b) [6].

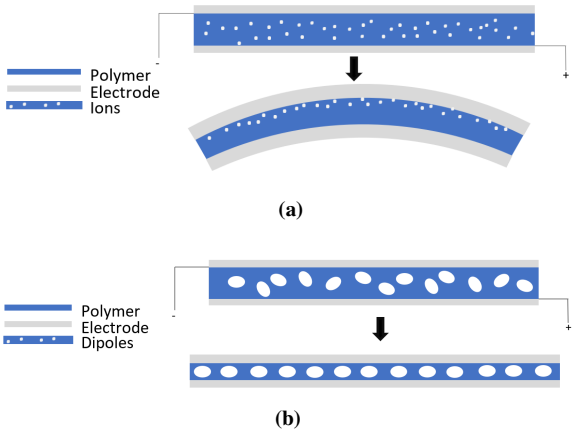

Figure 1: Schematic description of ionic polymers (a) and electronic polymer (b) under electric field activation

*[1]PIMM, Arts et Metiers ParisTech, CNRS, Cnam, HESAM Universite, 151 Bd de l'Hopital, 75013 Paris, France
†[2]Laboratoire de l'Integration du Materiau au Systeme (IMS, UMR 5218) 351 Cours de la Liberation, 33400 Talence, Cedex France.
‡[3] Arkema, CERDATO, Route du Rilsan, 27470 Serquigny, France

Thus, bending is produced by constraining the strain on one side with a passive substrate. Polypyrrole, for example, is a ionic EAP that has already been used for an endoscopic medical robot [7]. Although promising, since it requires low voltage actuation, it cannot maintain the resultant strain, exhibits a slow response time and induces a low actuation torque. Electronic EAPs have none of these shortcomings but require a high actuation voltage, which represents a major drawback for their implementation into real-life applications. To answer this issue, we propose a multilayered endoscopic actuator model which bypasses the high voltage problem of electronic EAPs. Due to the complexity of soft polymeric microstructures, analytical modeling will be performed to guide the experimental design and the fabrication of these electrostrictive based actuators (figure 2). While the smart materials move in a 2D plane, a roll mechanical actuation from the outside replaces the surgeon's wrist motion of the traditional endoscope.

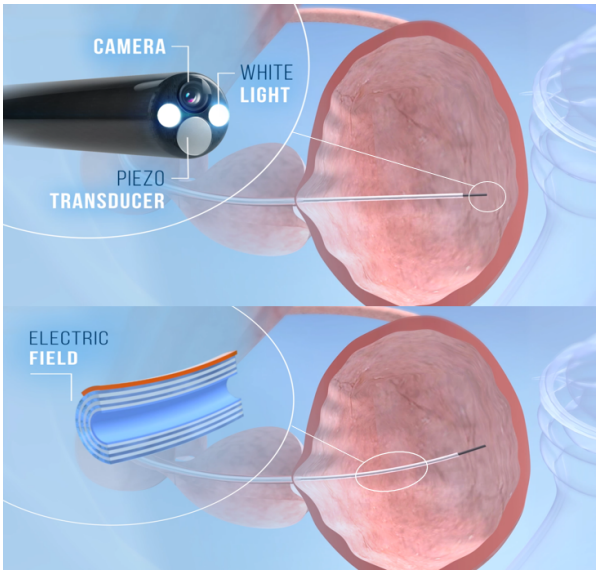

Figure 2: 3D design of a cystoscopic robot distal tip embedded materials and its EAP actuator integration in the structure

The number of parameters involved in the manufacturing of such an actuator is important (thickness, polymer formulation, passive materials composition, etc), making the craft manufacturing both time consuming and expensive. So, first, we therefor designed a theoretical model which enables the identification of the curvature behavior and corresponding bending force, we then used these results to develop an experimental prototype of the EAP actuator.

2. ANALYTICAL MODEL

Due to their bio compatibility, conformability of integration, low Young's modulus, high strain capabilities and relative low cost, EAPs are promising materials for the next generation of micro-scaled robotic components [8]. The electronic polymer studied in this paper is not a simple dielectric but also a relaxor ferroelectrics polymer. Those types of materials are recognized for their reversible large strain power. The terpolymer P(VDF-ter-TrFE-ter-CTFE), one such material, presents a high dielectric constant (50) and a high electrostrictive strain (4%). The third monomer CTFE introduction disrupts the conformation ordering of the chains into the ferroelectric crystal and creates a relaxor ferroelectric from a ferroelectric polymer. Under electrical field actuation, the so-created nano dipoles lines up in the field direction that results in a thickness diminution and a size increase in the two perpendicular directions. When constrained at one side by a passive material, the entire structure bends in one single direction under voltage actuation as depicted in figure 3.

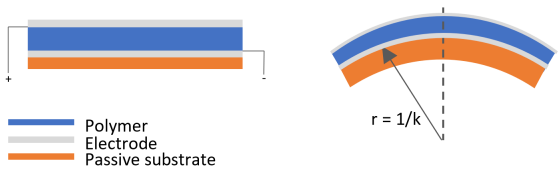

Figure 3: Schematic design of the bending composite structure with $r = \frac{1}{k}$ the radius of curvature

The EAP actuator is composed at least by three materials, the passive substrate, the terpolymer and two electrodes. The EAP is called multilayer if the following couple of materials, electrode-terpolymer, is repeated one after another as presented in figure 4.

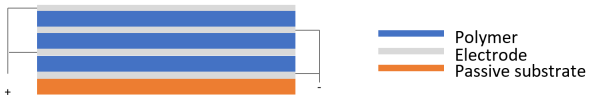

Figure 4: Schematic design of a multilayer composite material actuator

2.1. MECHANICAL BEHAVIOR

The EAP actuator is made of a composite multilayer material; the different layers are superimposed along the Z axis (figure 5). By considering orthotropic elastic materials, the strain behavior can be developed as follows:

$$\varepsilon_x^i(z) = \varepsilon_{0x} + \frac{z}{\rho_x} = \varepsilon_{0x} + zk_x \quad -t_s \leq z \leq t_e + n(t_e + t_p)$$
$$\varepsilon_y^i(z) = \varepsilon_{0y} + \frac{z}{\rho_y} = \varepsilon_{0y} + zk_y \quad -t_s \leq z \leq t_e + n(t_e + t_p)$$

ε_{0x} is the $z = 0$ strain and $k_x = \frac{1}{\rho_x}$ is the curvature in te X axis with ρ_x the radius of curvature (see figure 5). The Y axis strain is depicted on the same basis. $\varepsilon_{elastique} = \varepsilon_{total} - \varepsilon_{electrostrictif}$ and $\varepsilon_{electrostrictif} = M_i T^2$ with M_i is the electrostrictive constant matrix and T the electric field. The elastic strain is a function of ε_0 and k in every layer i. n is the number of active layers.

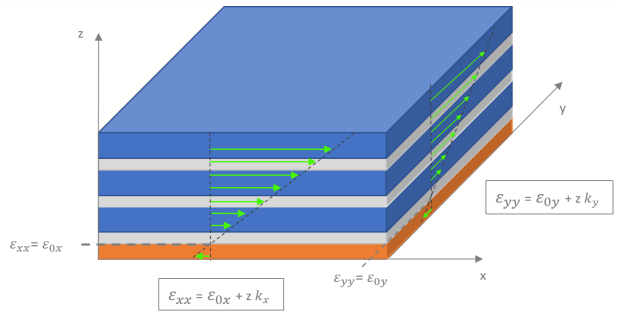

Figure 5: Schematic design of the strain in the composite material including the strain formula depending on the height z

$$^{el}\varepsilon_x^i(z) = \varepsilon_{0x} + zk_x - M_i T^2; \quad -t_s \leq z \leq t_e + n(t_e + t_p)$$
$$^{el}\varepsilon_y^i(z) = \varepsilon_{0y} + zk_y - M_i T^2; \quad -t_s \leq z \leq t_e + n(t_e + t_p)$$

For the EAP polymer layer $E_i = E_p$ is the Young's modulus and $M_i = M_p$ is the electrostrictive constant matrix. In the electrode layer, $E_i = E_e$ and $M_i = 0$. For a composite orthotropic material and based on [9], [10], the stress-strain relation is:

$$\begin{pmatrix} \sigma_x^i \\ \sigma_y^i \\ \tau_{xy}^i \end{pmatrix} = \begin{pmatrix} Q_{11}^i & Q_{12}^i & Q_{13}^i \\ Q_{12}^i & Q_{22}^i & Q_{23}^i \\ Q_{13}^i & Q_{23}^i & Q_{33}^i \end{pmatrix} \begin{pmatrix} ^{el}\varepsilon_x^i \\ ^{el}\varepsilon_y^i \\ ^{el}\gamma_{xy}^i \end{pmatrix} \quad (1)$$
$$= \frac{E_i}{1-\nu_i^2} \begin{pmatrix} 1 & \nu_i & 0 \\ \nu_i & 1 & 0 \\ 0 & 0 & \frac{1-\nu_i}{2} \end{pmatrix} \begin{pmatrix} ^{el}\varepsilon_x^i \\ ^{el}\varepsilon_y^i \\ ^{el}\gamma_{xy}^i \end{pmatrix} \quad (2)$$

Where, Q_{jk} are the plane stress reduced elastic constants in the plate axes of the i^{th} layer. We can introduce the resultant stress as:

$$\begin{pmatrix} N_x \\ N_y \\ N_{xy} \end{pmatrix} = \sum_{i=0}^{2n+2} \frac{E_i}{1-\nu_i^2} \begin{pmatrix} 1 & \nu_i & 0 \\ \nu_i & 1 & 0 \\ 0 & 0 & \frac{1-\nu_i}{2} \end{pmatrix} \int_{t(i)} \begin{pmatrix} ^{el}\varepsilon_x^i \\ ^{el}\varepsilon_y^i \\ ^{el}\gamma_{xy}^i \end{pmatrix} dz \quad (3)$$

With $t(i)$ the layer thickness depending on the material i.

$$\int_t {}^{el}\varepsilon_x dz = \int_{-t_s}^{0} {}^{el}\varepsilon_x^s dz + \int_0^{t_e+n(t_e+t_p)} {}^{el}\varepsilon_x^i dz \quad (4)$$

The resultant moment is written as follow:

$$\begin{pmatrix} M_x \\ M_y \\ M_{xy} \end{pmatrix} = \sum_{i=0}^{2n+2} \frac{E_i}{1-\nu_i^2} \begin{pmatrix} 1 & \nu_i & 0 \\ \nu_i & 1 & 0 \\ 0 & 0 & \frac{1-\nu_i}{2} \end{pmatrix} \int_{t(i)} \begin{pmatrix} ^{el}\varepsilon_x^i \\ ^{el}\varepsilon_y^i \\ ^{el}\gamma_{xy}^i \end{pmatrix} .zdz \quad (5)$$

Where t is the total thickness of the actuator in the Z axis.

$$\int_t {}^{el}\varepsilon_x .zdz = \int_{-t_s}^{0} {}^{el}\varepsilon_x^s .zdz + \int_0^{t_e+n(t_e+t_p)} {}^{el}\varepsilon_x^i .zdz \quad (6)$$

When no external stress or torque is applied on the system, we have $N_x = N_y = M_x = M_y = 0$. From this system of equation, we can highlight the k_x expression with the unknown parameters $\varepsilon_{0x}, \varepsilon_{0y}$ and k_y: $k_x = K.M_p.T^2$. This analytical model highlights the proportional behavior between curvature and electrostrictive terms. The curvature is directly related to the bending capacity but the K constant is a ratio of the geometrical parameters which is too complicated and then have to be studied with a Finite Element Model (FEM). Since this mechanical development is based on a linear geometrical assumption, it is effective for small strain and large displacement [11] and [12] but still the projection into the large bending axis has to be performed with a FEM software. The analytical model enables to understand the basic behavior of the composite material and to control the numerical model validity.

2.2. FINITE ELEMENT MODEL

Electrostrictive materials strain is a quadratic function of the electric field T. The electrostrictive material behavior is not implemented directly on Abaqus, the software we used for this study, so we had to use a thermal analogy [13].The model uses shell elements because of the difference between the length ($\approx 5cm$) and the thickness ($\approx 20\mu m$) of the actuator. Furthermore, a millimeter conversion has been done to avoid numerical issues due to values closed to zero. Table 1 reports the main conversions from SI to SI mm. We first studied the mesh size and type. From $6.10^{-3}m$ to $2.10^{-4}m$, shell quadratic elements S8R5 (figure 6 a) and shell linear elements S4R (figure 6 b) are both suitable for small strain and large displacements. Linear mesh S4R merges to a parabolic behavior as expected from the analytical model, except for the last mesh size, which diverges due to buckling. The S4R linear shell elements of $5.10^{-4}m$ will be used. The max strain is $2.10^{-6}m$ so the elements strain is under 0.5% .

Physical value	SI (m)	Factor	SI (mm)
Length	m	10^3	mm
Mass	Kg	10^{-3}	Tonne
Time	s	1	s
Electric intensity	A	1	A
Force (N)	$Kg.m.s^{-2}$	1	$Tonne.mm.s^{-2}$
Pressure (Pa)	$Kg.m^{-1}.s^{-2}$	10^{-6}	$Tonne.mm^{-1}.s^{-2}$
Density ($Kg.m^{-3}$)	$Kg.m^{-3}$	10^{-12}	$Tonne.mm^{-3}$
Voltage (V)	$Kg.m^2.A^{-1}.s^{-3}$	10^3	$Tonne.mm^2.A^{-1}.s^{-3}$
Electric field (V/m)	$Kg.m.A^{-1}.s^{-3}$	1	$Tonne.mm.A^{-1}.s^{-3}$
Energy (J)	$Kg.m^2.s^{-2}$	10^3	$Tonne.mm^2.s^{-2}$

Table 1: Conversion table from SI to SI millimeter

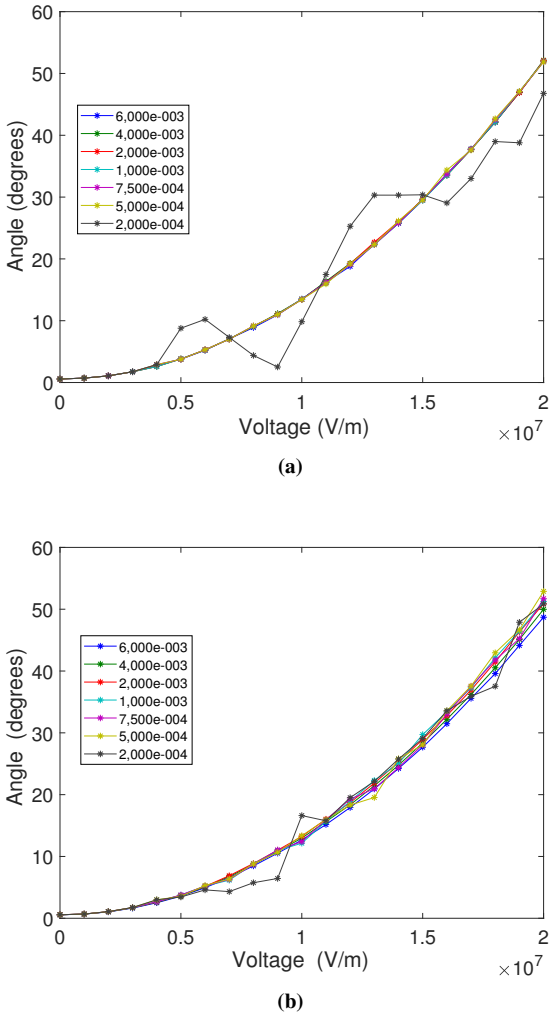

Figure 6: Mesh size and type influence on the angle of curvature depending on the electric field. With (a) S8R5 quadratic shell elements and (b) S4R linear shell elements

The figure 7 presents the visual motion results of bending capacity and induced force of a 50 mm x 4 mm rectangular actuator. The induced force in figure 7 b comes

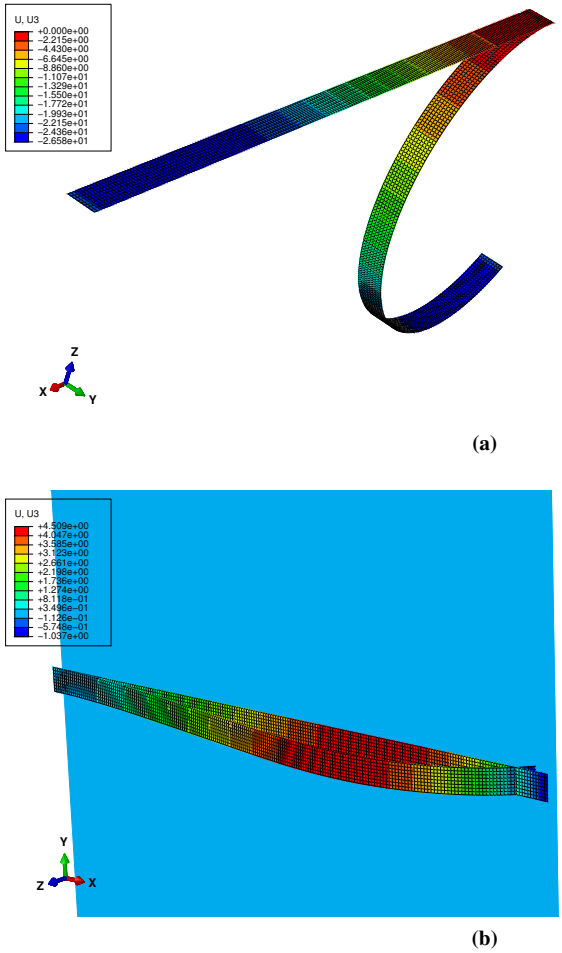

Figure 7: FEM visual motion results of the actuator bending (a) and of the actuator blocked by a 2D plane to generate the induced force (b) under voltage actuation

from the contact between the actuator and a 2D plane (in blue). A parametric study was performed to characterize the influence of all the parameters on the curvature and induced force. The analysis is made from a standard model based on the experimental test bench. The bending is measured by the angle $\theta = ks/2$ with k being the curvature. The curvature appears constant all along the actuator length s. As expected, to perform a suitable bending, the actuator needs to be soft and thin, as depicted in figure 8. It appears that increasing the voltage could counteract this trend, but once again voltage is limited by the maximum receivable electric field in the active materials. The terpolymer Young's modulus is not studied because the active material composition can not be changed. The electrostrictive coefficient is set to $3.10^{-18} m^2/V^2$ as in the manufacturer data sheet.

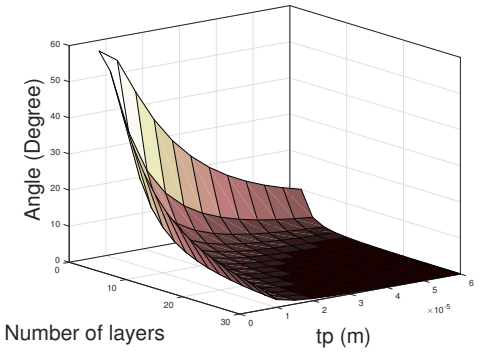

(a)

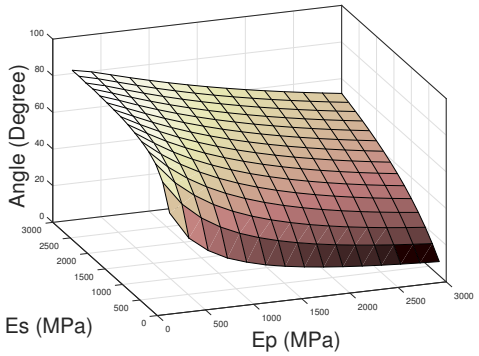

(b)

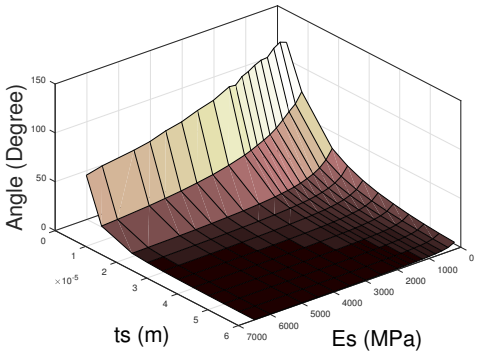

(c)

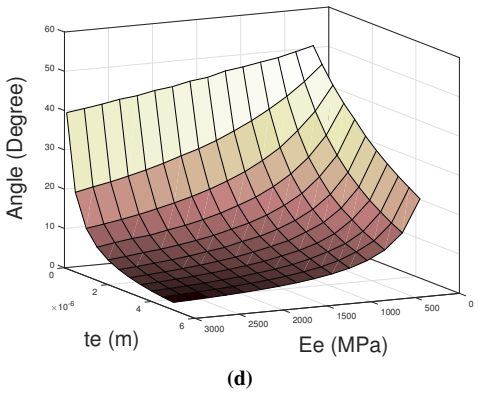

(d)

Figure 8: Parametric study of the actuator bending angle depending on (a) the number of layers and the active layers thickness tp (b) the passive substrate and the electrodes' Young's modulus Ee and Ep (c) the passive substrate Young's modulus Ep and thickness tp (d) the electrodes' Young's modulus Ee and thickness te

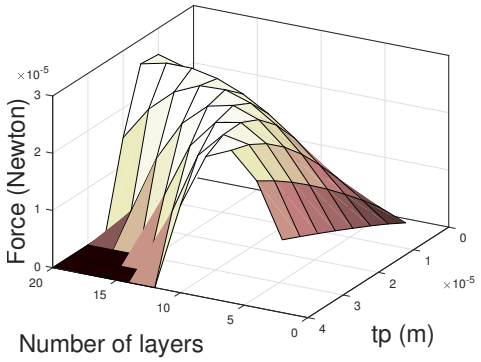

(a)

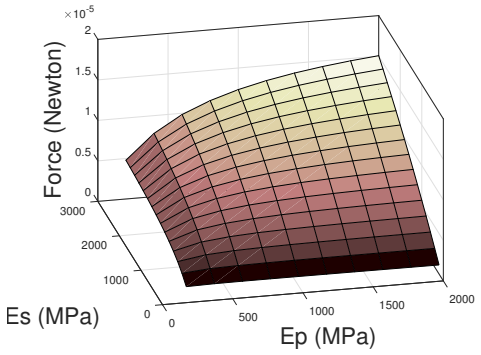

(b)

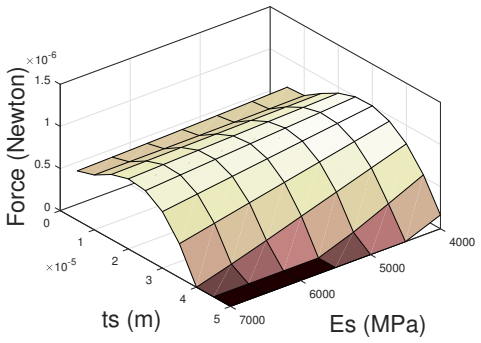

(c)

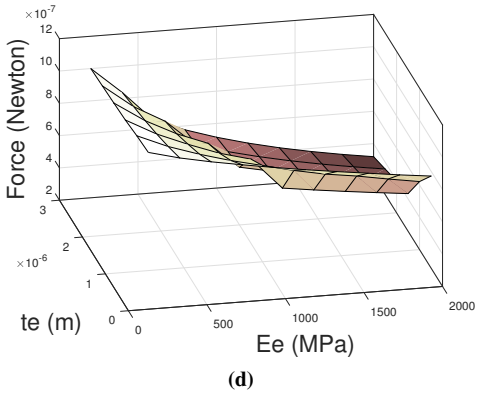

(d)

Figure 9: Parametric study of the actuator induced force depending on (a) the number of layers and the active layers thickness tp (b) the passive substrate and the electrodes' Young's modulus Ee and Ep (c) the passive substrate Young's modulus Ep and thickness tp (d) the electrodes' Young's modulus Ee and thickness te

The parametric study presented in figure 9 of the induced force shows something different than the parametric study of the bending capacity. Indeed the stiffer the material the bigger the induced force. Global stiffness can be achieved whith high thickness and high Young's modulus. Finally a twenty layer actuator could reach the targeted attributes both for bending and induced force by not using thick layers or strong materials. However, multilayer devices are quite difficult to manufacture. Another solution in order to improve stiffness could be to make a cylindrical shape actuator as proposed in [14]. This solution would require another experimental process and make the parametric analysis more complicated. Furthermore a better understanding of the contact between layers could result in a FEM improvement and a meta model is actually being studied by our group to enable an extrapolation in a larger range of parameters.

3. EXPERIMENTAL ANALYSIS

A screen printing machine was used in a clean room to print micrometer and nanometer layers. A PEN (PolyEthylene Naphtalate) film substrate of $25\mu m$ is used as a support. The EAP is made of terpolymer P(VDF-ter-TrFE-ter-CTFE) provided by Piezotech S.A.S (Arkema group, France). Those inks materials are spread on the screen with stainless blades before being annealed (figure 10). The electrodes' material is also a polymer because of its low Young's modulus and fusion temperature around the terpolymer's temperature to avoid the EAP liquefaction. It is also printed from an ink with a $200\mu m$ mesh tissue screen. Larger layers, (from $10\mu m$ to $50\mu m$) can be printed using a stencil printing method. This process is quite similar to the previous one except for the use of a non meshed stainless steel screen.

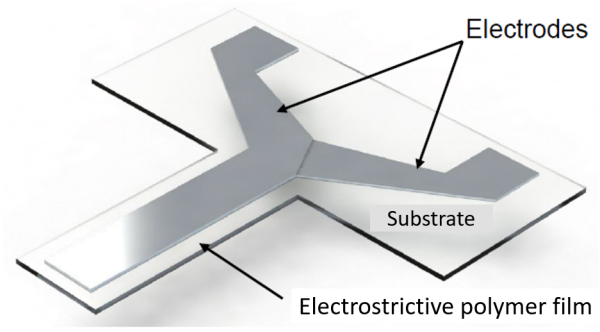

Figure 10: Schematic design of the experimental composite material

Table 2: Actuator parameters

Part	Material	Young's Modulus	Thickness
Substrate	PEN	0.2 GPa	25 μm
Electrode	PEDOT:PSS	0.02 GPa	200 nm
EAP	P(VDF-TrFE-CTFE)	0.2 GPa	$6\mu m$
Electrode	PEDOT:PSS	0.02 GPa	200 nm

For the prototype described in table 2 we have made a test bench to put the device under electric actuation. In figure 11, we can see that the process leads to a 110 degree bending angle at $180V/\mu m$. This shows that the radius of curvature appears non-constant, certainly because of typical manufacturing defects. We have also recorded an actuation inherent threshold of $50V/\mu m$. We observed that the control accuracy reached one degree per ten volts with perfect repeatability. Figure 11 depicts the qualitative comparison of the experimental and numerical analysis including the threshold correction. The main trend is similar in both models which gives credit to the FEM. Figure 12 confirms that the

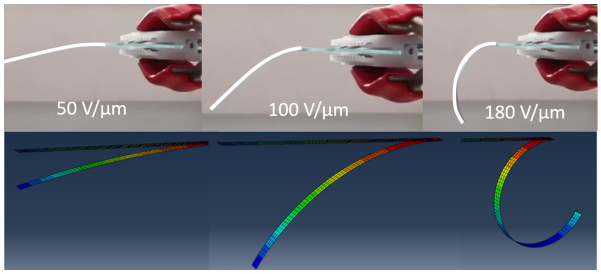

Figure 11: Bending capacity of the composite actuator describe in the table 2 both experimental and numerical

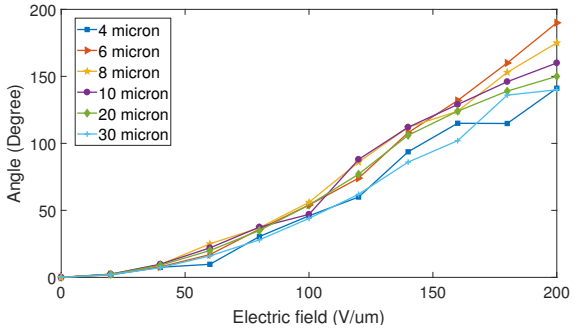

Figure 12: Influence of the terpolymer thickness over the bending capacity from the experimental model

bending capacity decreases as the terpolymer thickness increases. The difference in behavior for the 4 μm batch can be explained by the non homogeneity of the terpolymer at this level of thickness. Indeed, during the

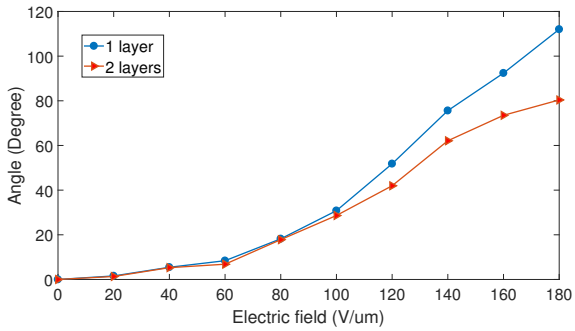

Figure 13: Influence of the terpolymer number of layers over the bending capacity from the experimental model

first actuation, air bubbles in the EAP material create holes resulting in local breakdowns if the material is too small, which reduces its bending capacity. The same phenomenon has also been observed for the multilayer devices. The air bubbles cross the electrodes to reach the second EAP material and break the actuator down. However a two-layer actuators was finally successfully printed with no native defaults. It consists of two-layers of EAP, three electrode layers and one passive substrate. Each EAP layer is $10\mu m$ thin. Figure 13 shows that as expected from the FEM, the bending capacity is lower for the two-layer actuator compared to the single-layer one. This multilayer EAP is still tougher and should induce a bigger force.

To summarize, the experimental study conducted by the FEM results have lead to the development of a successful prototype in terms of bending capacity. Also, the actuator perfectly holds the strain while under voltage and the accuracy is good enough to make it suitable for a robotic actuator. Repeatability was also tested and the actuator is able to go back to the same position for a known value of voltage. Also a two-active-layer actuator was successfully manufactured. This accomplishment passes the way to the experimental design of more than two-layer actuators in order to perform both bending and to induce a force. At the moment processing issues have to be solved while the know-how skills are still acquired.

4. CONCLUSION

EAP's and especially electronic ones are promising materials for robotic components. However, to enable their common use we needed to understand their behavior when they are combined with other materials as a composite actuator. In that aim, we have developed a numerical model to understand the influence of multiple parameters and guide the physical experiments. This model has shown promising results in terms of bending capacity and induced force prediction and will be completed by a metamodel to extend its workspace. Based on the FEM analysis, we have designed a real composite actuator batch by using a screen printing method. This actuator has shown great results especially in terms of bending capacity and control accuracy. While a two-layer actuator has successfully been manufactured, an electronic EAP-based endoscopic robot would need an important force, requiring more layers, which is the main difficulty of its fabrication. Besides, this model could be improved by adding fluid structure interactions, organ tissue friction and by using another geometrical shape (ex: cylinder). This numerical and experimental work will also provide data for the control theory. Traditional discreet joint actuators and rigid link robots descriptions are not applicable for soft robots since continuum actuators are part of the robot shape, as studied in [15], [16] and [17]. In the future, soft endoscopic robots made of smart electro-mechanical structures could replace poly-articulated traditional tools and provide full automated or teleoperated surgical solutions in the area of non-invasive surgery.

ACKNOWLEDGMENT

This research was supported by Piezotech S.A.S (Arkema group, France), Laboratoires Coloplast (Coloplast group, Denmark) and Tenon Hospital Urology service (France).

References

[1] Jianzhong Shang, David P. Noonan, Christopher Payne, James Clark, Mikael Hans Sodergren, Ara Darzi, and G.-Z. Yang. An articulated universal joint based flexible access robot for minimally invasive surgery. In *Robotics and Automation (ICRA), 2011 IEEE International Conference on*, pages 1147–1152. IEEE, 2011.

[2] Avi Friedman, Alex Liberzon, and Gabor Kósa. Propulsive force of a magnetic, MRI-based swimmer. In *Robotics and Automation (ICRA), 2015 IEEE International Conference on*, pages 4736–4741. IEEE, 2015.

[3] Hao Su, Weijian Shang, Gregory Cole, Gang Li, Kevin Harrington, Alexander Camilo, Junichi Tokuda, Clare M. Tempany, Nobuhiko Hata, and Gregory S. Fischer. Piezoelectrically Actuated Robotic System for MRI-Guided Prostate Percutaneous Therapy. *IEEE/ASME Transactions on Mechatronics*, 20(4):1920–1932, August 2015.

[4] Yili Fu, Hao Liu, Wentai Huang, Shuguo Wang, and Zhaoguang Liang. Steerable catheters in minimally invasive vascular surgery. *The International Journal of Medical Robotics and Computer Assisted Surgery*, 5(4):381–391.

[5] Y. Bar-Cohen. Electroactive polymers (EAP) as actuators for potential future planetary mechanisms. In *Proceedings. 2004 NASA/DoD Conference on Evolvable Hardware, 2004.*, pages 309–317, Seattle, WA, USA, 2004. IEEE.

[6] Lei Zhu. Exploring Strategies for High Dielectric Constant and Low Loss Polymer Dielectrics. *The Journal of Physical Chemistry Letters*, 5(21):3677–3687, November 2014.

[7] Mohamed Taha Chikhaoui, Kanty Rabenorosoa, and Nicolas Andreff. Kinematics and performance analysis of a novel concentric tube robotic structure with embedded soft micro-actuation. *Mechanism and Machine Theory*, 104:234–254, October 2016.

[8] Mohiuddin Ahmed and Md. Masum Billah. Smart Material-Actuated Flexible Tendon-Based Snake Robot. *International Journal of Advanced Robotic Systems*, 13(3):89, June 2016.

[9] B N Pandya and T Kant. Finite Element Analysis of Laminated Composite Plates using a Higher-Order Displacement Model. page 19.

[10] T. Kant, C.P. Arora, and J.H. Varaiya. Finite element transient analysis of composite and sandwich plates based on a refined theory and a mode superposition method. *Composite Structures*, 22(2):109–120, January 1992.

[11] Anil Erol, Sarah Masters, Paris von Lockette, and Zoubeida Ounaies. On the Modeling and Experimental Validation of Multi-Field Polymer-Based Bimorphs. In *Volume 1: Multifunctional Materials; Mechanics and Behavior of Active Materials; Integrated System Design and Implementation; Structural Health Monitoring*, page V001T01A014, Stowe, Vermont, USA, September 2016. ASME.

[12] Mary I Frecker and William M Aguilera. Analytical modeling of a segmented unimorph actuator using electrostrictive P(VDF-TrFE) copolymer. *Smart Materials and Structures*, 13(1):82–91, February 2004.

[13] C.H. Hsueh. Thermal stresses in elastic multilayer systems. *Thin Solid Films*, 418(2):182–188, October 2002.

[14] Jean-Fabien Capsal, Jeremy Galineau, Minh-Quyen Le, Fabrice Domingues Dos Santos, and Pierre-Jean Cottinet. Enhanced electrostriction based on plasticized relaxor ferroelectric P(VDF-TrFE-CFE/CTFE) blends. *Journal of Polymer Science Part B: Polymer Physics*, 53(19):1368–1379, October 2015.

[15] Robert J. Webster, Allison M. Okamura, and Nah J. Cowan. Toward active cannulas: Miniature snake-like surgical robots. In *Intelligent Robots and Systems, 2006 IEEE/RSJ International Conference on*, pages 2857–2863. IEEE, 2006.

[16] Deepak Trivedi, Christopher D. Rahn, William M. Kier, and Ian D. Walker. Soft robotics: Biological inspiration, state of the art, and future research. *Applied Bionics and Biomechanics*, 5(3):99–117, December 2008.

[17] B.A. Jones and I.D. Walker. A New Approach to Jacobian Formulation for a Class of Multi-Section Continuum Robots. In *Proceedings of the 2005 IEEE International Conference on Robotics and Automation*, pages 3268–3273, Barcelona, Spain, 2005. IEEE.